0026-895X/92/010120-07$03.00/0

MOLECULAR PHARMACOLOGY, 41:120-126

Slow Voltage-Dependent Block of Sodium Channels in Crayfish Nerve by Dihydropyrazole Insecticides

VINCENT L. SALGADO*

Rohm and Haas Company, Spring House, Pennsylvania 19477

Received July 19, 1991; Accepted October 14, 1991

SUMMARY

Previous current-clamp work has shown that dihydropyrazole insecticides block sodium channels in tonic sensory receptors and in axons depolarized by high K^+ external solutions and that hyperpolarization removes the block [*Pestic. Sci.* **28**:389–411 (1990)]. Voltage-clamp studies on internally perfused crayfish giant axons were done to confirm and extend these observations. At −100 mV dihydropyrazoles had little effect on the sodium current, but at more depolarized potentials they blocked it from either face of the membrane. The onset of block following a holding potential change or during wash-in of a dihydropyrazole was very slow, with a time constant of several minutes, and, although block could be removed with a similar time course by hyperpolarization, the effects of the insecticides could not be reversed by prolonged washing. Dihydropyrazoles did not affect delayed rectifier potassium currents in the axon. The voltage-dependent block could be described as a uniform shift of the steady state (slow) sodium inactivation (S_∞) curve in the direction of hyperpolarization, indicative of selective binding to inactivated states of the channel. Using hyperpolarizing prepulses to remove slow inactivation, block of sodium channels by dihydropyrazoles could be measured directly at holding potentials as positive as −50 mV, and it could be demonstrated that block saturated near −70 mV, consistent with a dependence on slow inactivation. The data were fit to a model that assumes the dihydropyrazole binds to the slow-inactivated state of the channel on a one to one basis. Dissociation constants obtained from this analysis were similar to those obtained from analysis of inhibition of the binding of [*benzoyl*-2,5-^{3}H]-batrachotoxinin A 20-α-benzoate by the same dihydropyrazoles. In axons whose fast or slow inactivation gates had been removed by *N*-bromoacetamide or trypsin, respectively, dihydropyrazoles still blocked sodium current, indicating that dihydropyrazoles can block the channel as well as enhance the normal slow inactivation process.

Dihydropyrazoles are a class of experimental broad-spectrum neurotoxic insecticides with a novel mode of action. A previous study (1) showed that dihydropyrazoles block neural activity in insects, leading to paralysis. Tonic sensory nerves were especially sensitive to the blocking action. Current-clamp studies on the crayfish slowly adapting stretch receptor and the crayfish giant axon showed that the nerve-blocking action of dihydropyrazoles was due to voltage-dependent block of sodium channels, with block being enhanced by depolarization and inhibited by hyperpolarization (1), leading to the hypothesis that dihydropyrazoles bind to the 'anticonvulsant' binding site (2) on the voltage-dependent sodium channel (1). This hypothesis is supported by the recent finding that dihydropyrazoles allosterically inhibit the binding of BTX-B to rat brain synaptoneurosomes (3) and show reciprocal competitive interactions with veratridine and batrachotoxin in $^{22}Na^+$ uptake studies (4). The present paper investigates the interaction of dihydropyrazoles with sodium channels in crayfish giant axons under voltage clamp, confirming the voltage-dependent blocking action. The results indicate that the action of dihydropyrazoles on sodium channels is similar to that of local anesthetics, class I anticonvulsants, and class I antiarrhythmics (2), but with kinetics that are several orders of magnitude slower.

Materials and Methods

Crayfish (*Procambarus clarkii*) giant axons were voltage clamped with the axial wire method modified from Ref. 5, with solutions based on Ref. 6. The nerve cord was dissected from ganglion 2 (subesophageal ganglion) to ganglion 10 (numbered according to Ref. 5) and placed in an ice-cooled Plexiglas chamber in potassium-free external solution (210 NaVH) (Table 1) for desheathing and cleaning. During cleaning, the nerve cord was held taut between two clips with no. 8 silk suture, in such a way that it could be rotated on its axis. The medial giant axon on one side was cleaned of adhering fibers, especially between ganglia 6 and 9, which would be in the current-measuring region. The other side of the cord was left intact for support, connected to the cleaned axon by tufts of connecting fibers in the region of the ganglia. Although it was often possible to obtain good preparations from isolated

* Present address: Dow Elanco Discovery Research, P.O. Box 708, Greenfield, IN 46140

ABBREVIATIONS: [^{3}H]BTX-B, [*benzoyl*-2,5-^{3}H]batrachotoxinin A 20-α-benzoate; CsIS, cesium-containing internal solution; SIS, standard internal solution; I_K, potassium current; I_{Na}, sodium current; NBA, *N*-bromoacetamide; VH, van Harreveld.

axons, the success rate was improved with the partial cleaning described. The circumesophageal connectives (between ganglia 1 and 2) are more easily dissected than the portion of the nerve cord between ganglia 2 and 10, and the giant axon is usually of the greatest and most uniform diameter in that region, making it suitable for use in the sucrose-gap voltage-clamp method (7). However, the axon was invariably leaky in the region of ganglion 2, making it impossible to obtain a long enough stretch of good axon in this region for the axial wire method.

The cleaned nerve cord was transferred to a Plexiglas voltage-clamp chamber and aligned parallel to, and within 100 μm from, three platinized platinum plate electrodes, a 2-mm-wide central current-measuring electrode flanked by a 5-mm guard on either side (refer to Ref. 5 for diagram). A perfusion cannula pulled from glass capillary tubing was inserted at one end of the cleaned axon, between ganglia 9 and 10, and the axon was tied to it with no. 10 silk suture. The other end of the nerve cord was pulled around two posts made from 10-mil silver wires glued to the bottom of the chamber, and the suture tied to that end was fixed to the outside wall of the chamber with Tackiwax (Central Scientific Co.), after the region of the axon between ganglia 7 and 8 was positioned near the central platinum plate. A slit was made in the axon where it rounded the bend around the first silver post, and the internal perfusion was begun with a pressure head of 3–4 cm. Often, momentary application of higher pressure was needed to get perfusion started.

The internal electrode was of the piggy-back design, consisting of a 25-μm Pt-10% Ir wire glued to a capillary that had been pulled to about 40 μm from larger tubing (World Precision Instruments No-Fil, 1.0 mm). A stiff copper wire soldered to the tip of a soldering iron provided localized heat to attach the wire to the capillary with hot-melt craft glue. The capillary was long enough so that the tip could reach the center of the current-measuring electrode, and the wire protruded 6 mm past it to reach the end of the further guard electrode. The wire was platinized for the last 12 mm (6 mm along the capillary and 6 mm beyond it), except for a small region near the capillary tip where the two were glued. Finally, a 10-μm Pt-10% Ir wire was platinized and inserted into the capillary from the very tip to the shank, to reduce the high frequency impedance of the electrode. This internal wire was essential for a rapid voltage-clamp system. The capillary and an external reference electrode that was positioned near the axon in the current-measuring region were filled with 1 M KCl and connected to a voltage-clamp circuit with Ag/AgCl pellet electrodes.

All experiments were carried out with potassium-free external (210 NaVH) solution and either SIS or a potassium-free internal solution (CsIS) (Table 1). However, to avoid depolarization of the axon, the internal perfusion was always begun with SIS until the voltage was clamped.

The temperature was 16°, unless otherwise noted. Insecticides (Fig. 1) were synthesized at Rohm and Haas Company (8, 9) and stored at −20° in dimethyl sulfoxide, from which they were diluted into the test solution. Insecticides were applied in the internal solution, but their activity did not differ markedly when applied externally. The concentration of dimethyl sulfoxide in the test solutions was always <0.1%, which had no effect on the ionic currents of the axon.

TABLE 1
Solution composition

Component	Composition		
	210 NaVH	SIS	CsIS
		mM	
NaCl	210	15	0
$CaCl_2$	10	0	0
K-Glutamate	0	170	0
KF	0	50	0
CsF	0	0	50
Cs-Glutamate	0	0	170
HEPES	2	5	5
pH	7.5	7.35	7.35

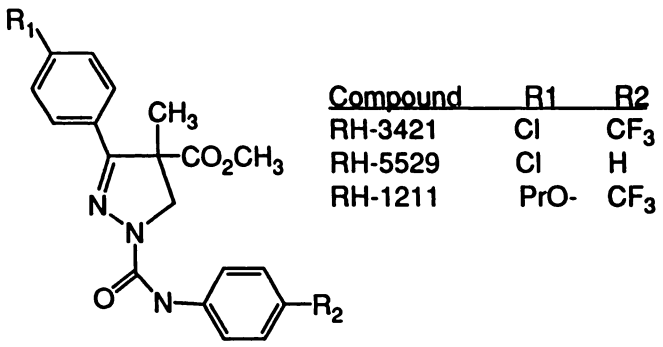

Fig. 1. Chemical structures of the dihydropyrazoles discussed in this paper.

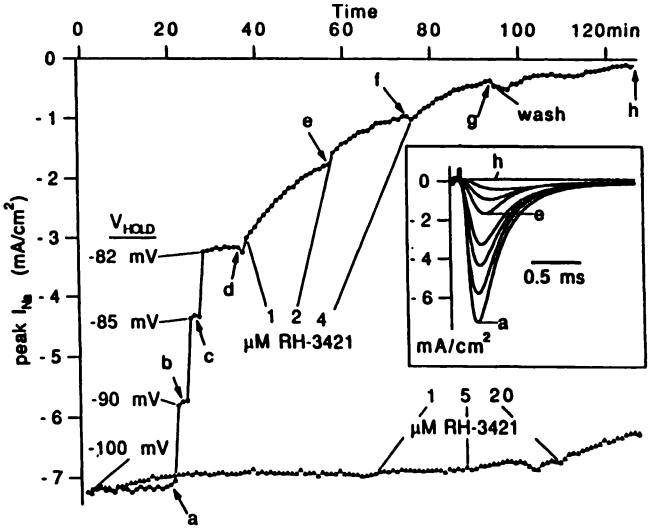

Fig. 2. Dihydropyrazoles block I_{Na} only in depolarized axons. *Circles*, peak I_{Na} from an axon whose holding potential was depolarized stepwise from −100 to −82 mV in the period between 20 and 40 min, causing peak I_{Na} to decrease >50% due to the normal process of inactivation. Peak I_{Na} held steady at −82 mV and was sensitive to block by RH-3421, which was not readily reversed by washing. Sample I_{Na} traces, corresponding to the *arrows* in the *main figure*, are shown in the *inset*. *Triangles*, peak I_{Na} from another axon, which was held at −100 mV for the duration and responded much more weakly to RH-3421, consistent with the hypothesis that dihydropyrazole block is voltage dependent. Experiment W8804.

Binding of [^{3}H]BTX-B (New England Nuclear) to rat brain synaptoneurosomes was determined at 37° in the presence of *Leiurus quinquestriatus* venom (Sigma catalogue no. V5251), by the methods of Deecher *et al.* (3) for mouse brain, except that volumes used in the preparation of synaptoneurosomes were scaled up by a factor of 3 in going from mouse to rat. For binding inhibition studies, dihydropyrazoles were dissolved in ethanol and added to the incubation mixture. Each assay tube (120-μl total volume) contained approximately 110 μg of protein, 11 μg of *Leiurus* venom (sufficient to give near-maximal enhancement of [^{3}H]BTX-B binding), 10 nM [^{3}H]BTX-B, and 0.5% ethanol as the solvent for the dihydropyrazoles. Samples were incubated for 1 hr and harvested individually on Whatman GF/C glass fiber filters, using a filter manifold. Treatments were done in duplicate, and nonspecific binding determined in the presence of 500 μM veratridine was subtracted, to obtain specific binding.

Results

At a holding potential of −100 mV, concentrations of RH-3421 as high as 20 μM had very little effect on the sodium current (Fig. 2, *triangles*). When the holding potential was reduced to −82 mV (Fig. 2, *second point after c*), peak inward current decreased rapidly due to sodium inactivation, after which it remained stable. However, at this depolarized potential, as little as 1 μM RH-3421 caused substantial block (Fig. 2, *second point after d*). The onset of block was slow, taking longer than 20 min to reach steady state. Furthermore, washout was difficult to demonstrate (Fig. 2). The time course of sodium currents was not affected by RH-3421. The slight prolongation of the time to peak I_{Na} for the currents in Fig. 2 (*inset*) was due to uncompensated series resistance and was also seen when the current was reduced with depolarizing prepulses or with tetrodotoxin. The other dihydropyrazoles used in this study, RH-5529 and RH-1211, had similar effects on I_{Na}, depressing it at depolarized holding potentials without changing its time course.

Sensitivity of the sodium current to dihydropyrazoles clearly depended on membrane potential and could arise from selective binding to an inactivated state of the channel. Sodium channels undergo two kinetically distinct types of inactivation. Under the present conditions, fast inactivation, measured with the two-pulse protocol (10) with a 30-msec conditioning pulse, had a midpoint at −61 ± 4 mV and a slope of *e*-fold in 7.3 ± 1.3 mV (mean ± standard deviation), whereas slow inactivation, measured at steady state, as in Fig. 2, had a midpoint at −80 ± 3 mV and changed *e*-fold in 4.5 ± 0.4 mV (mean ± standard deviation) (Table 2; an example is shown in Fig. 3).

Because the voltage sensitivity of dihydropyrazole action appears in the range over which slow inactivation occurs, which is about 20 mV more negative than fast inactivation (Table 2), it seems that the dihydropyrazole may bind selectively to the slow-inactivated state. In the remainder of this paper, S_∞ will be used to represent steady state slow inactivation. In a number of experiments similar to Fig. 2, in which dihydropyrazoles were washed in at constant voltage, block was measured after 20 min and plotted against S_∞; there was a clear relationship (Fig. 4).

TABLE 2

Parameters of steady state slow and fast inactivation

V_h is the half-point for inactivation and k is the slope in mV per *e*-fold change in inactivation. Parameters were obtained by nonlinear regression to eq. 1 (Appendix).

Expt.	Slow V_s	Slow k	Fast V_h	Fast k	Fast − slow, $V_h - V_s$
			mV		
V8721	−80.2	4.4			
W8721	−77.7	4.5			
V8722	−80.1	4.7			
V8726	−81.0	4.3			
V8824	−76.9	3.8			
W8803	−85.2	4.4	−65.8	5.8	19.4
W8804	−83.0	4.5	−64.4	6.0	18.6
V8804	−87.0	4.6	−66.1	7.1	20.9
V8805	−78.8	4.4	−55.1	5.8	23.7
V8923	−77.9	5.1	−64.4	7.4	13.5
V8928	−76.5	3.8	−55.1	7.8	21.4
V8930	−78.5	4.4	−58.3	9.5	20.2
V8O06	−81.4	4.9	−61.9	9.1	19.5
V8O07	−79.6	4.8	−59.7	7.2	19.9
Mean	−80.3	4.5	−61.2	7.3	19.7
SD	3.1	0.4	4.3	1.3	2.7

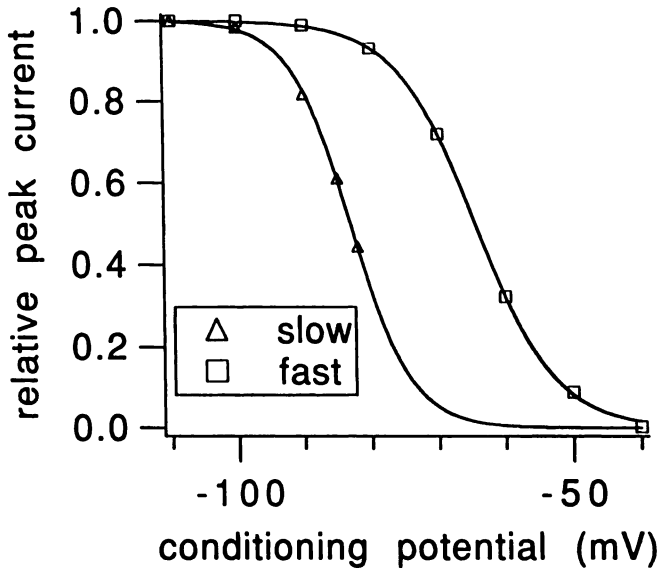

Fig. 3. Steady state fast and slow inactivation relations for sodium current measured with conditioning pulses of 30 msec and several minutes, respectively. Parameters V_h, V_S, and k, as defined in the Appendix, were estimated by nonlinear regression of eq. 1 to the data. Experiment W8804.

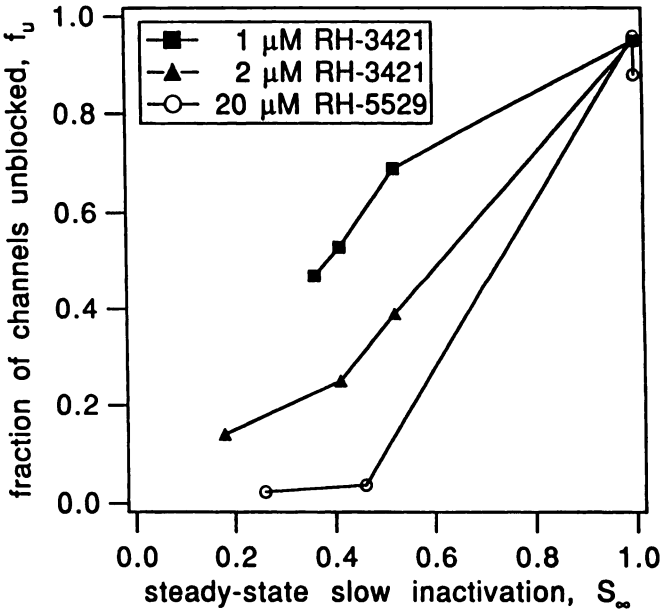

Fig. 4. Dihydropyrazole block is correlated with slow sodium inactivation. Block of I_{Na} by dihydropyrazoles at constant voltage is plotted versus the steady state slow inactivation parameter, S_∞, which is the ratio of peak I_{Na} at a given holding potential to its maximum value at a very negative holding potential (−120 mV).

The degree of block of the sodium current by a given concentration of a dihydropyrazole could be modulated by varying the holding potential. Before treatment (Fig. 5, 0–50 min), step changes in holding potential resulted in rapid changes of steady state inactivation. Application of 10 μM RH-3421 at −75 mV led to nearly total block of I_{Na}, but restoration of the holding potential to −120 mV led to recovery of most of it. Subsequent steps to various holding potentials led to varying degrees of block. The failure of peak I_{Na} at −120 mV to recover completely

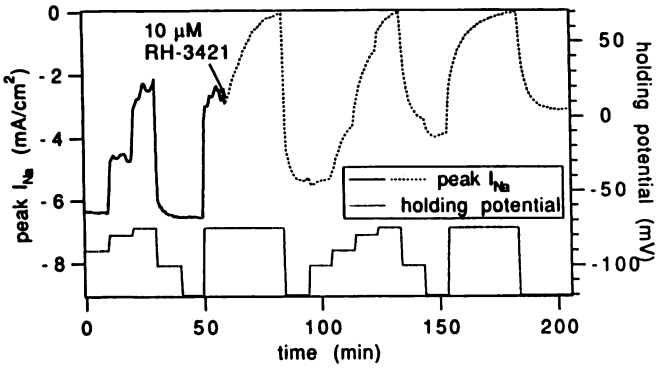

Fig. 5. Dihydropyrazole block can be modulated by varying holding potential. When peak I_{Na} was measured at 30-sec intervals, step changes in holding potential before treatment resulted in rapid changes in steady state inactivation, as seen in this figure up to about 50 min. Application of 10 μM RH-3421 at −75 mV led to nearly total block of I_{Na}, but restoring the holding potential to −120 mV led to recovery of most of it. Subsequent depolarizing holding potential steps starting at about 100 min led to slow onset of block, and repolarizing steps led to slow recovery. The failure of peak I_{Na} at −120 mV to recover completely to its original level was due more to rundown than to residual block. Experiment V8824.

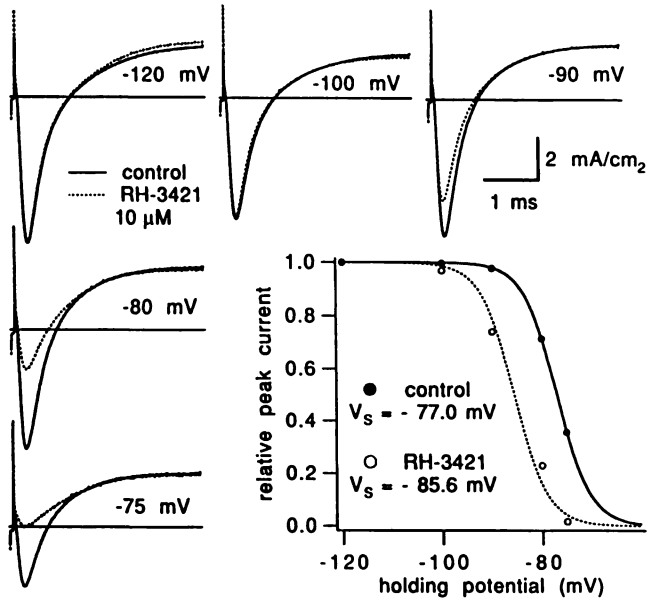

Fig. 6. Dihydropyrazole block appears as a parallel shift of the steady state slow inactivation curve in the direction of hyperpolarization. Ionic current traces from the experiment of Fig. 5 (traces after treatment were scaled by a common factor so that the peak at −120 mV matched the peak before treatment, to compensate for rundown) show that, after treatment with the dihydropyrazole, peak I_{Na} was depressed most at depolarized potentials, whereas outward current, I_K, was not affected by the treatment. The graph shows plots of peak current normalized to the value at −120 mV. RH-3421 (10 μM) appears to shift this steady state inactivation relation to the left by 8.6 mV. Experiment V8824.

to its original level was due more to rundown than to residual block.

Selected ionic current traces from the experiment in Fig. 5 are shown in Fig. 6. Both sodium and potassium components are present, because SIS was used internally. To compensate for rundown, the traces obtained after treatment were normalized so that the peak at −120 mV after treatment matched the peak before treatment. After treatment, peak I_{Na} was depressed most at depolarized potentials, whereas I_K was not significantly

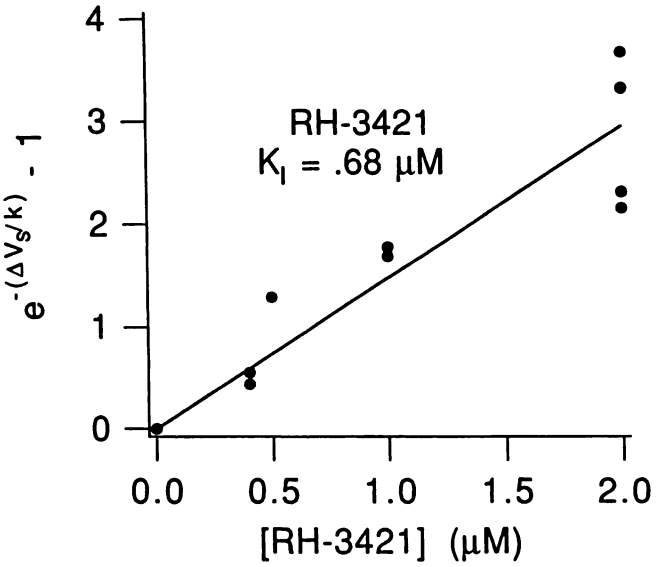

Fig. 7. Inactivation voltage shift follows relation predicted by the model in the Appendix. The shift of the midpoint of the steady state inactivation curve, ΔV_S, produced by various concentrations of RH-3421 in crayfish axons follows eq. 2 (Appendix) reasonably well. The reciprocal of the slope of the regression line gives K_I = 0.68 ± 0.06 μM for RH-3421.

changed. The graph shows the steady state S_∞ curves derived by plotting the peak inward currents at various holding potentials, normalized to their values at −120 mV. RH-3421 at 10 μM appears to shift the steady state inactivation relation to the left by 8.6 mV. A shift in S_∞, which will be denoted by ΔV_S, has been previously observed with lidocaine block of cardiac sodium channels and was interpreted as selective binding of the drug to the inactivated state (11). The shifts of V_s in various concentrations of RH-3421 are plotted in Fig. 7, according to eq. 2 (Appendix); the regression line estimates a dissociation constant of 0.68 μM for binding of RH-3421 to the inactivated state of the sodium channel. The fact that the line extrapolates to zero at zero dihydropyrazole concentration supports the hypothesis that it is slow and not fast inactivation that is responsible for the enhancement of dihydropyrazole binding in these experiments.

The model in the Appendix predicts that binding of dihydropyrazoles to sodium channels is voltage dependent only in the voltage range over which slow inactivation occurs, so that at strong depolarizations, where inactivation is complete, further depolarization should not lead to further block. When peak current was measured as a function of holding potential, as in Figs. 5 and 6, inactivation prevented measurement of the voltage dependence of block at strong depolarizations.

In order to observe block directly at strong depolarizations, where inactivation is substantial, the axon was held at various potentials, as in previous experiments, but a hyperpolarizing prepulse to −120 mV was applied just before the test pulse. A 500-msec hyperpolarizing prepulse was used, which was adequate to remove slow inactivation (Fig. 8) without interfering with block, which recovered much more slowly (on the order of minutes). The protocol, which measures the fraction of channels not blocked by the dihydropyrazole (f_u), is shown in Fig. 9A, *inset*. The graph in Fig. 9A shows the time course of block following steps from −120 mV to various other potentials (with reequilibration at −120 mV between runs), in an axon equilibrated with 1 μM RH-1211. The time course and steady state

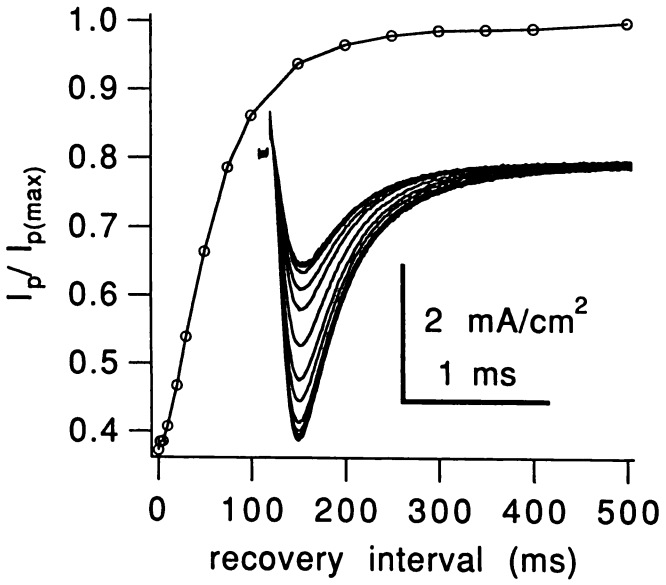

Fig. 8. Time course of recovery from slow inactivation of the sodium current after changing the holding potential from −75 to −120 mV. Recovery was complete well before 500 msec, which is the recovery interval used in Fig. 9. Experiment V8014.

level of block were independent of holding potential between −70 and −50 mV. Steady state block from this axon and another one treated with 0.5 μM RH-1211 is plotted in Fig. 9B. The solid curves were plotted according to eq. 3 (Appendix), with $K_I = 0.14$ μM, $V_S = -78.2$ mV, and $k = 4.44$ mV, and agree very well with the data. These inactivation parameters are very close to the averages for slow inactivation (Table 2), adding further support for the hypothesis that the dihydropyrazole binds to the slow-inactivated rather than the fast-inactivated state under the conditions of the experiment.

The results up to this point quantitatively support the model in the Appendix and so are consistent with the hypothesis that the dihydropyrazoles bind selectively to the slowly inactivated state of the sodium channel. It is also possible that dihydropyrazoles bind to other channel states, such as the open and fast-inactivated states, but these events could not be measured here, because of the slow kinetics of binding. Local anesthetics can bind to and block open channels when the inactivation gate is removed by internal perfusion with Pronase (12, 13).

Because the kinetics of interaction of dihydropyrazoles with sodium channels are so much slower than those of local anesthetics, we must look at the effects of both fast and slow inactivation gates on the ability of dihydropyrazoles to block the channels. The pulse protocol shown in Fig. 10, *inset A*, was used to observe the two types of inactivation, fast and slow, and their removal by internal perfusion of NBA (14) and trypsin (15), respectively. At depolarized holding potentials, in the absence of a 500-msec hyperpolarizing prepulse, slow inactivation was seen as a reduction of peak I_{Na} (Fig. 10, *inset B, dashed trace*). Brief perfusion of 0.02 mg/ml trypsin removed slow inactivation (Fig. 10, *inset C*) but left fast inactivation largely intact; subsequent treatment with 1 mM NBA (Fig. 10, *inset D*) resulted in axons with neither slow nor fast inactivation. Neither of these treatments reduced the effectiveness of RH-1211 in blocking I_{Na} (Fig. 10, *main graph*). This result suggests that the dihydropyrazole can bind to the channel and inhibit ion conduction in the absence of inactivation gates.

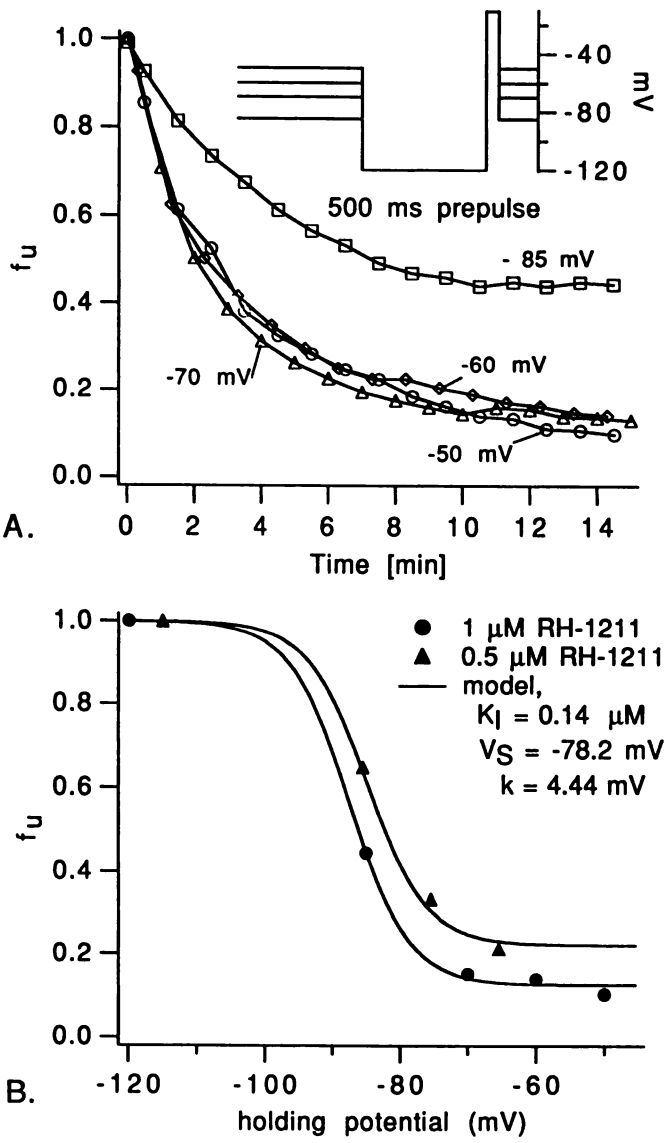

Fig. 9. Block is asymptotic at strong depolarizations. The model in the Appendix predicts that block of Na^+ channels by dihydropyrazoles is voltage dependent only in the range over which inactivation occurs. In order to observe block directly at strong depolarizations, where inactivation is complete, the axon was held at various potentials as in previous experiments, but a 500-msec hyperpolarizing prepulse to −120 mV was applied just before the 10-msec test pulse to −10 mV, during which I_{Na} was measured (see *inset* protocol). The prepulse was of sufficient amplitude and duration to remove inactivation completely (Fig. 8), without interfering with block. A, Time course of f_u, the fraction of channels unblocked, following steps from −120 mV to various other potentials, in an axon equilibrated with 1 μM RH-1211. Steady state block from this and another axon treated with 0.5 μM RH-1211 are plotted in B. The *solid curves* in B were plotted according to eq. 2, with $K_I = 0.14$ μM, $V_h = -78.2$ mV, and $k = 4.44$ mV.

This finding does not imply that the dihydropyrazole binds to states other than inactivated states. In the ball-and-chain model of inactivation (16–18), removal of the ball with trypsin or NBA need not alter the voltage dependence of the conformational changes in the membrane-associated segments of the channel. Binding of dihydropyrazoles may still require the inactivated conformation, even though the channel is not occluded by the ball.

Dihydropyrazoles inhibit the binding of [^{3}H]BTX-B to

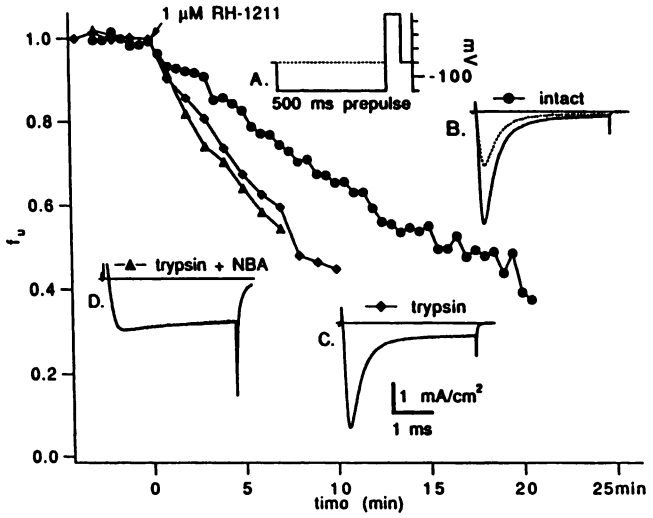

Fig. 10. Intact inactivation gates are not required for block by dihydropyrazoles. The pulse protocol shown in *inset A* was used to observe the two types of inactivation, fast and slow, and their removal by internal perfusion of NBA and trypsin, respectively. At depolarized holding potentials, in the absence of a 500-msec hyperpolarizing prepulse, slow inactivation is seen as a reduction of peak I_{Na} (*inset B, dashed trace*). Brief perfusion of 0.02 mg/ml trypsin removed slow inactivation (*inset C*) but left fast inactivation largely intact; subsequent treatment with 1 mM NBA (*inset D*) also removed fast inactivation. Neither of these treatments reduced the effectiveness of RH-1211 in blocking I_{Na}. This result suggests that the dihydropyrazole can bind to states other than the inactivated state(s) and that this binding can inhibit ion conduction even in the absence of inactivation gates.

TABLE 3

Comparison of the dissociation constants for RH-3421 and RH-1211, determined in the crayfish axon by voltage clamp (K_i) and in rat brain synaptoneurosomes by inhibition of binding of [^{3}H]BTX-B

For rat brain, IC_{50} values were determined by nonlinear regression, and K_d values were calculated from IC_{50} values by the Cheng-Prusoff formula (19). Numbers in parentheses define the 95% confidence interval for K_d.

Compound	K_d	
	Crayfish axon	Rat brain
		μM
RH-3421	0.68	0.27 (0.262–0.282)
RH-1211	0.14	0.10 (0.098–0.111)

mouse brain synaptoneurosomes with a Hill coefficient near 1, indicating a one to one binding reaction (3). Similar results were obtained in the present study with rat brain synaptoneurosomes (data not shown). Table 3 compares the dissociation constants for RH-3421 and RH-1211 derived from the voltage-clamp data in Figs. 7 and 9, respectively, with K_d values derived from [^{3}H]BTX-B binding. There is an excellent correspondence, considering the different species and methods used.

Discussion

The results reported here have confirmed that dihydropyrazoles block sodium channels in a voltage-dependent manner. Equilibrium block is quantitatively consistent with the assumption that dihydropyrazoles bind selectively to an inactivated state of the channel on a one to one basis, as has been proposed for local anesthetics (11). Kinetically, dihydropyrazoles bind much more slowly than do local anesthetics, so use dependence is not evident, and time-dependent block is not seen during single voltage-clamp pulses, even when inactivation is removed by trypsin and NBA.

Because of its very slow kinetics, binding of dihydropyrazoles could be demonstrated only to the slowly inactivated state, but binding to other states is not excluded. The only state that dihydropyrazoles have been shown not to bind to at toxicologically relevant concentrations is the resting state. When slow or fast inactivation was removed with trypsin or NBA, respectively, RH-1211 was still able to block sodium channels (Fig. 10), indicating that it could bind to states that were not inactivated but that, nevertheless, may be different from the normal open state.

A recent study of the effects of the dihydropyrazole RH-3421 on the binding of [^{3}H]BTX-B to mouse brain synaptoneurosomes supports the hypothesis that dihydropyrazole binding is state dependent (3). In that study, RH-3421 allosterically inhibited the binding of [^{3}H]BTX-B, at concentrations where it did not enhance the rate of dissociation of the ligand from its receptor. Because [^{3}H]BTX-B binds selectively to an activated state of the channel, failure of RH-3421 to enhance dissociation at concentrations near its K_d indicates that the dihydropyrazole does not bind strongly to the BTX-bound activated state (20).

The voltage-clamp studies reported here show that the binding of RH-3421 to sodium channels is very slowly reversible in response to voltage changes (Fig. 5), so the failure to obtain recovery with washout (Fig. 2) (Fig. 9 of Ref. 1) is probably due to the difficulty of washing the compound out of the membrane. The fact that the lipophilic dihydropyrazoles had similar activity from either side of the membrane suggests that their site of action is within the membrane and accessible through the lipid phase, as is also thought to be the case for local anesthetics (21).

The state dependence of the action of the dihydropyrazoles described here provides an explanation of the sensitivity of tonic sensory receptors to their action (1). When firing tonically, such cells are operating near their thresholds, in the voltage range over which inactivation occurs, making their sodium channels available to bind dihydropyrazoles. The voltage dependence of inactivation of sodium channels in the spike-generating region of a tonic sensory receptor must be markedly different from that of axonal sodium channels, because the crayfish slowly adapting stretch receptor neuron can generate action potentials at −60 mV (1), whereas axonal sodium channels are fully inactivated at that potential (Fig. 3). Interestingly, interaction of RH-5529 with sodium channels in a crayfish sensory neuron was readily reversible within a couple of minutes (Fig. 9 of Ref. 1), whereas in giant axons of the same species the same compound required almost 60 min for washout (Fig. 16 of Ref. 1). Slow wash-in and washout of RH-5529 was also observed in the present experiments under voltage clamp. The molecular features of the channel that give rise to these differences in inactivation may also be responsible for differences in kinetics of dihydropyrazole binding.

The excellent correspondence between the potency of dihydropyrazoles in crayfish axon voltage-clamp studies and rat brain [^{3}H]BTX-B binding studies suggests that the binding site is similar in both species. Furthermore, there is a good correlation between insecticidal potency and potency in displacing [^{3}H]BTX-B from rat brain sodium channels.[1]

[1] V. L. Selgado, Unpublished observations.

There is direct evidence that sodium channel block is the relevant target site of dihydropyrazoles in insects (1), but similar evidence is lacking in mammals. The $^{22}Na^+$ flux studies of Deecher and Soderlund (4) showed that the compounds do inhibit sodium flux through sodium channels in mammalian synaptoneurosomes, and Nicholson and co-workers (22, 23) found that dihydropyrazoles inhibited release of neurotransmitters from synaptosomes prepared from both guinea pig brain and cricket nerve cords. Dietary RH-3421 caused a delayed onset neurological syndrome in rats, including symptoms of ataxia, tremors, lethargy, and convulsions,[2] but there are as yet no data linking sodium channel block with this syndrome.

Acknowledgments

I thank R. M. Jacobson for synthesizing the dihydropyrazoles used in this study and R. A. Nicholson and D. M. Soderlund for communicating the results of their studies before publication.

Appendix

The Na^+ channel undergoes transitions between many different conformations or states, which can be grouped into resting (R), open (O), and inactivated (I) states, each of which may have several substates. The observed negative shift of S_∞ (Fig. 6) suggests that the dihydropyrazole, D, binds selectively to an inactivated state and not to the resting state.

In this simplified model, $S_\infty = [R]/([R] + [I])$ is the steady state slow inactivation parameter, which depends on membrane potential according to:

$$S_\infty = \frac{1}{1 + \exp((V - V_S)/k)} \quad (1)$$

where V is membrane potential, V_S is the potential at which $S_\infty = 0.5$, and k is a constant. $K_I = [D] \times [I]/[D \cdot I]$ is defined as the equilibrium dissociation constant of the D·I complex. State O is not present at equilibrium and can be ignored in this analysis.

When block is measured with no hyperpolarizing prepulse, peak I_{Na} is proportional to the fraction of channels in state R, $[R]/([R] + [I] + [D \cdot I])$, from which it can be shown algebraically that the dihydropyrazole will shift the S_∞ versus V relation by an amount ΔV_S, where:

$$e^{-\Delta VS/k} - 1 = \frac{[D]}{K_I} \quad (2)$$

When channels in state I are made to return to the resting state with a hyperpolarizing prepulse (Fig. 9), peak I_{Na} during the subsequent test pulse is proportional to the fraction of channels in states R and I, $([R] + [I])/([R] + [D \cdot I] + [I])$, which is equal to the fraction of channels unblocked, f_u. f_u can be shown to depend on both V and [D], according to the relation:

$$f_u = \frac{1}{1 + \frac{[D]}{K_I}\left(\frac{1}{1 + \exp((V_S - V)/k)}\right)} \quad (3)$$

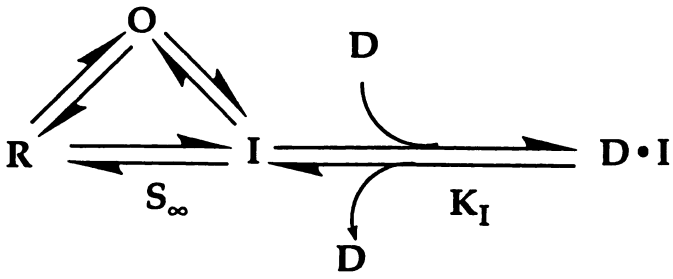

[2]Rohm and Haas Company Toxicology Department, unpublished observations.

References

1. Salgado, V. L. Mode of action of insecticidal dihydropyrazoles: selective block of impulse generation in sensory nerves. *Pestic. Sci.* **28**:389–411 (1990).
2. Catterall, W. A. Common modes of drug action on Na^+ channels: local anesthetics, antiarrhythmics and anticonvulsants. *Trends Pharmacol. Sci.* **8**:57–65 (1987).
3. Deecher, D. C., G. T. Payne, and D. M. Soderlund. Inhibition of [^{3}H] batrachotoxinin A 20-α-benzoate binding to mouse brain sodium channels by the dihydropyrazole insecticide RH-3421. *Pestic. Biochem. Physiol.* **41**:265–273 (1991).
4. Deecher, D. C., and D. M. Soderlund. RH-3421, an insecticidal dihydropyrazole, inhibits sodium channel-dependent sodium uptake in mouse brain preparations. *Pestic. Biochem. Physiol.* **39**:130–137 (1991).
5. Shrager, P. Ionic conductance changes in voltage clamped crayfish axons at low pH. *J. Gen. Physiol.* **64**:666–690 (1974).
6. Lund, A. E., and T. Narahashi. Modification of sodium channel kinetics by the insecticide tetramethrin in crayfish giant axons. *Neurotoxicology* **2**:213–229 (1981).
7. Salgado, V. L., J. Z. Yeh, and T. Narahashi. Use- and voltage-dependent block of the sodium channel by saxitoxin. *Ann. N. Y. Acad. Sci.* **479**:84–95 (1986).
8. Jacobson, R. M. Insecticidal *N*-aryl-3-aryl-4,5-dihydro-1*H*-pyrazole-1-carboxamides. United States Patent No. 4,663,341 (1987).
9. Jacobson, R. M. *N*-Aryl-3-aryl-4,5-dihydro-1*H*-pyrazole-1-carboxamides and methods of their production. United States Patent No. 4,863,947 (1989).
10. Hodgkin, A. L., and A. F. Huxley. The dual effect of membrane potential on sodium conductance in the giant axon of *Loligo*. *J. Physiol. (Lond.)* **116**:497–506 (1952).
11. Bean, B. P., C. J. Cohen, and R. W. Tsien. Lidocaine block of cardiac sodium channels. *J. Gen. Physiol.* **81**:613–642 (1983).
12. Yeh, J. Z., and T. Narahashi. Kinetic analysis of pancuronium interaction with sodium channels in squid axon membranes. *J. Gen. Physiol.* **69**:293–323 (1977).
13. Yeh, J. Z. Dynamics of 9-aminoacridine block of sodium channels in squid axons. *J. Gen. Physiol.* **73**:1–21 (1979).
14. Oxford, G. S., C. H. Wu, and T. Narahashi. Removal of sodium channel inactivation in squid giant axons by *N*-bromoacetamide. *J. Gen. Physiol.* **71**:227–247 (1978).
15. Starkus, J. G., and P. Shrager. Modification of slow sodium inactivation in nerve after internal perfusion with trypsin. *Am. J. Physiol.* **255**:C238–C244 (1978).
16. Armstrong, C. M., and F. Bezanilla. Inactivation of the sodium channel. II. Gating current experiments. *J. Gen. Physiol.* **70**:567–590 (1977).
17. Zagotta, W. N., T. Hoshi, and R. W. Aldrich. Restoration of inactivation in mutants of Shaker potassium channels by a peptide derived from ShB. *Science (Washington D. C.)* **250**:533–538 (1990).
18. Hoshi, T., W. N. Zagotta, and R. W. Aldrich. Biophysical and molecular mechanisms of Shaker potassium channel inactivation. *Science (Washington D. C.)* **250**:533–538 (1990).
19. Cheng, Y.-C., and W. Prusoff. Relationship between the inhibition constant (K_I) and the concentration of inhibitor which causes 50 per cent inhibition (I_{50}) of an enzymatic reaction. *Biochem. Pharmacol.* **22**:3099–3108 (1973).
20. Hill, R. J., H. J. Duff, and R. S. Sheldon. Class I antiarrhythmic drug receptor: biochemical evidence for state-dependent interaction with quinidine and lidocaine. *Mol. Pharmacol.* **36**:150–159 (1989).
21. Hille, B. Local anesthetics: hydrophobic and hydrophilic pathways for the drug-receptor reaction. *J. Gen. Physiol.* **69**:497–515 (1989).
22. Nicholson, R. A., and E. Merletti. The effect of dihydropyrazoles on release of [^{3}H]GABA from nerve terminals isolated from mammalian cerebral cortex. *Pestic. Biochem. Physiol.* **37**:30–40 (1990).
23. Nicholson, R. A., and C. O. Kumi. The effects of pesticides, brevetoxin B, and the cardiotonic drug DPI 201 106 on release of acetylcholine from insect central nerve terminals. *Pestic. Biochem. Physiol.* **40**:86–97 (1991).

Send reprint requests to: Dr. Vincent L. Salgado, DowElanco Discovery Research, P.O. Box 708, Greenfield, IN 46140.